Organic & Biomolecular Chemistry

ROYAL SOCIETY OF CHEMISTRY

PAPER

View Article Online
View Journal | View Issue

Cite this: *Org. Biomol. Chem.*, 2025, **23**, 3366

Stabilization of optically inactive α-helices of peptidic foldamers through sequence control and *i*, *i* + 4 stapling†

Naoki Ousaka, *[a,b] Mark J. MacLachlan, *[b,c,d] Shigehisa Akine *[b,e] and Shigenori Fujikawa *[a,f,g]

We report the effect of a minimal (*i*, *i* + 4) staple on the dynamic interconversion between right-handed (*P*) and left-handed (*M*) forms of an optically inactive α-helical peptide composed only of helicogenic achiral amino acids, such as 1-amino-cyclohexanecarboxylic acid (Ac_6c) and 4-aminopiperidine-4-carboxylic acid (Api) residues. The *P*/*M* interconversion rate of the peptide with a flexible hydrocarbon-based staple was estimated to be 0.41 s^{-1} at 298 K through variable temperature ^{1}H NMR measurements in 1,1,2,2-tetrachloroethane-d_2. A combined analysis using ^{1}H NMR spectroscopy, single-crystal X-ray crystallography, and density functional theory (DFT) calculations revealed that the present flexible stapling does not effectively constrain the conformational freedom of the helical peptide. DFT calculations revealed that Ac_6c residues exhibit a stronger propensity for α-helical conformation over the 3_{10}-helix than α-aminoisobutyric acid (Aib) residues, with their influence being highly dependent on position and sequence within the oligopeptides.

Received 11th February 2025,
Accepted 4th March 2025

DOI: 10.1039/d5ob00244c

rsc.li/obc

Introduction

The stabilization of the α-helical conformation of short oligopeptides has attracted much attention because of its potential therapeutic application.[1–5] Among the methods for such stabilization, intramolecular cross-linking between peptide side chains, *i.e.* stapling, is one of the powerful strategies to stabilize the helical conformation not only of α-helical peptides[1–8] but also of helical polymers[9–11] and oligomers (foldamers) composed of abiotic backbones.[12–16] It is also known that the incorporation of strongly helicogenic chiral or achiral C^α-tetrasubstituted amino acid residues into oligopeptides instead of naturally occurring C^α-trisubstituted ones stabilizes 3_{10}- or α-helical conformations of peptides.[17–21] When only achiral C^α-tetrasubstituted amino acids, such as α-aminoisobutyric acid (Aib),[17,22,23] 1-amino-cyclohexanecarboxylic acid (Ac_6c),[24–26] and 4-aminopiperidine-4-carboxylic acid (Api),[27,28] are used to build oligopeptides, the achiral peptides fold into racemic mixtures of both right-handed (*P*) and left-handed (*M*) helices in a 1 : 1 molar ratio. For example, homo-Aib oligomers are known to adopt a dynamically racemic 3_{10}-helical conformation rather than the corresponding α-helical one, most likely due to a strong 3_{10}-helical propensity of the Aib residues,[18,22,29–31] and to undergo rapid interconversion between enantiomeric (*P*)- and (*M*)-forms on the millisecond time scale.[32–36] This rapid interconversion rate of Aib-based 3_{10}-helical peptides can be reduced by a factor of approximately 10^6 through a single staple between the side chains of Api residues introduced at the *i*th and *i* + 3th positions, which are located on the same side of the 3_{10}-helix.[37,38] Similar to these 3_{10}-helices, we have recently reported stapled α-helical peptides that exhibit a slow interconversion between (*P*)- and (*M*)-forms on a time scale of minutes.[39] These peptides are composed mainly of Ac_6c and its piperidine analog Api residues, with intramolecular cross-linking between the side chains of the Api residues introduced at the *i*th and *i* + 7th

[a]*Research Center for Negative Emissions Technologies, Kyushu University, 744 Moto-oka, Nishi-ku, Fukuoka 819-0395, Japan. E-mail: ousaka.naoki.565@m.kyushu-u.ac.jp*
[b]*Nano Life Science Institute (WPI-NanoLSI), Kanazawa University, Kakuma-machi, Kanazawa 920-1192, Japan*
[c]*Department of Chemistry, University of British Columbia, 2036 Main Mall, Vancouver, BC, V6T 1Z1, Canada. E-mail: mmaclach@chem.ubc.ca*
[d]*Quantum Matter Institute, University of British Columbia, 2355 East Mall, Vancouver, BC, V6T 1Z4, Canada*
[e]*Graduate School of Natural Science and Technology, Kanazawa University, Kanazawa 920-1192, Japan. E-mail: akine@se.kanazawa-u.ac.jp*
[f]*International Institute for Carbon-Neutral Energy Research (WPI-I^{2}CNER), Kyushu University, 744 Moto-oka, Nishi-ku, Fukuoka, 819-0395, Japan. E-mail: fujikawa.shigenori.137@m.kyushu-u.ac.jp*
[g]*Department of Applied Chemistry, Graduate School of Engineering, Kyushu University, 744 Moto-oka, Nishi-ku, Fukuoka, 819-0395, Japan*

† Electronic supplementary information (ESI) available. CCDC 2421064 (**1C$_7$**). For ESI and crystallographic data in CIF or other electronic format see DOI: https://doi.org/10.1039/d5ob00244c

positions using a biphenyl-based cross-linker spanning two α-helical turns. Their *P*/*M* interconversion can be almost completely suppressed by introducing double staples, effectively transforming dynamic α-helices into static ones. Thanks to this static nature, doubly stapled α-helical peptides synthesized exclusively from achiral components can be separated into enantiomeric (*P*)- and (*M*)-α-helices using chiral HPLC. Moreover, the *P*/*M* interconversion rate is highly dependent on the stiffness of the staple moiety;[40] for instance, replacing the biphenyl-based staple with a more flexible hydrocarbon staple significantly accelerates the *P*/*M* interconversion of the corresponding α-helical peptides. While (*i*, *i* + 7) staples spanning two α-helix turns have been employed in Ac_6c-based peptides to construct both dynamic and static α-helical peptides,[39,40] the effect of a minimal stapling – *i.e.*, an (*i*, *i* + 4) staple spanning one α-helical turn-on the *P*/*M* interconversion of optically inactive α-helical peptides remains unknown. In addition, the helix type propensity (3_{10} *vs.* α-helix) of Ac_6c residues compared to that of Aib residues is still poorly understood.[24,25] Herein, we report the synthesis and structural characterization of an Ac_6c/Api-based nonapeptide with an (*i*, *i* + 4) staple and investigate the effect of minimal stapling on its *P*/*M* interconversion (Fig. 1). In addition, we also report a density functional theory (DFT)-based theoretical study that examines the effect of peptide chain length in homo-Ac_6c and alternative Aib-Ac_6c sequences on the 3_{10}-/α-helix propensities, as well as the effects of sequence and position of Ac_6c residues within Aib-based helical oligopeptides.

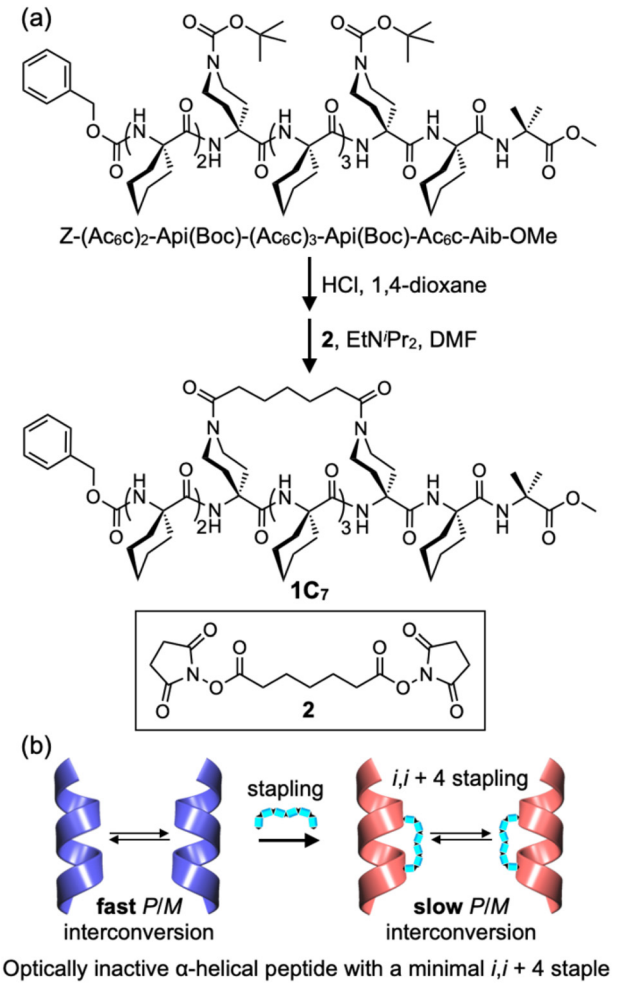

Fig. 1 (a) Synthesis of the stapled optically inactive α-helical peptide $\mathbf{1C_7}$ with an (*i*, *i* + 4) hydrocarbon-based staple. (b) Schematic representation of the deceleration of *P*/*M* interconversion in an optically inactive α-helical peptide upon minimal (*i*, *i* + 4) stapling.

Results and discussion

Theoretical study of 3_{10}-/α-helix type propensities of the Ac_6c and Aib residues

In the previous study, oligopeptides containing a tetrameric or hexameric homo-Ac_6c segment were found to undergo 3_{10}/α-helix transitions in response to solvent changes, with 3_{10}- and α-helical conformations induced in less polar $CHCl_3$ and polar 2,2,2-trifluoroethanol (TFE), respectively.[41] In sharp contrast, oligopeptides composed mainly of alternative $(Aib\text{-}Ac_6c)_n$ sequences (n = 4 and 8) did not adopt an α-helical conformation, even in TFE.[42] To gain further insight into the 3_{10}/α-helix type propensity of Ac_6c residues in optically inactive helical peptides, we performed DFT calculations to estimate the energy differences ($\Delta E_{\alpha\text{-}310}$ per residue, where $\Delta E_{\alpha\text{-}310} = E_\alpha - E_{310}$, in kJ mol^{-1}) between α- and 3_{10}-helical conformations of $\text{-}(Ac_6c)_n$- and $\text{-}(Aib\text{-}Ac_6c)_m$-based helical peptides with varying repeat numbers (Fig. 2). The $\Delta E_{\alpha\text{-}310}$ per residue values for acetyl-$(Ac_6c)_n$-$NHCH_3$ (n = 6) and acetyl-$(Aib\text{-}Ac_6c)_m$-Aib-$NHCH_3$ (m = 3) were positive, indicating their preferred formation of the 3_{10}-helix. In sharp contrast, when the peptide chain length was sufficiently long ($n \geq 7$ and $m \geq 4$), the α-helical conformation became energetically favored over the 3_{10}-helix. Moreover, the α-helix formation propensity of homo-Ac_6c peptides was significantly stronger than that of alternative Aib-Ac_6c peptides, consistent with the experimental observations described above (Fig. 2).[41,42]

Next, we estimated the $\Delta E_{\alpha\text{-}310}$ and the $\Delta E_{\alpha\text{-}310}/n$ (where n is number of Ac_6c residues, in kJ mol^{-1}) values of the optically inactive helical nonapeptides **I**–**IX**, acetyl-$(AA)_9$-$NHCH_3$ (AA = Ac_6c and/or Aib), with different amino acid sequences listed in Table 1, to clarify the effects of the number and position of Ac_6c residues in Aib-based nonapeptides on α-helix formation. Interestingly, replacement of the Aib(7) residue (the number in parentheses represents the residue number from the N-terminus) of acetyl-$(Aib\text{-}Ac_6c)_4$-Aib-$NHCH_3$ (**I**) with Ac_6c resulted in a significant increase in α-helical preference (peptides **I** and **II** in Table 1). This effect was further enhanced when the Aib(5) residue in peptide **II** was also substituted with Ac_6c (peptides **II** and **III** in Table 1). However, the further replacement of the Aib(3) residue in peptide **III** with Ac_6c, as well as its combination with Ac_6c substitutions at both termini produced only a relatively modest enhancement of α-helical preference compared to the previous substitutions. These

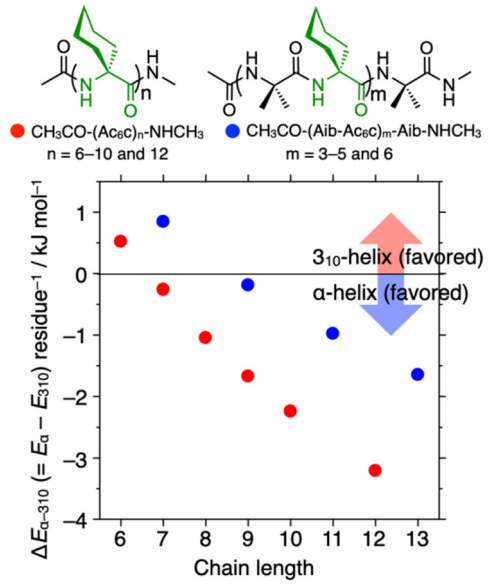

Fig. 2 Plots of the energy difference ($\Delta E_{\alpha\text{-}310}$ per residue, where $\Delta E_{\alpha\text{-}310} = E_{\alpha} - E_{310}$, in kJ mol^{-1}) between the α- and 3_{10}-helical conformations of acetyl-$(Ac_6c)_n$-$NHCH_3$ (n = 6, 7, 8, 9, and 12) (red circles) and acetyl-(Aib-$Ac_6c)_m$-Aib-$NHCH_3$ (m = 3, 4, 5, and 6) (blue circles) *versus* peptide chain length.

results suggest that segments composed of more than three consecutive Ac_6c residues strongly promote α-helical conformation in the corresponding nonapeptides. Additionally, peptide **VI** which contains two Ac_6c residues at the ith and i + 3th positions, destabilizes the 3_{10}-helical conformation, likely due to steric repulsion between the Ac_6c side chains. Similarly, Ac_6c substitutions at the ith and i + 4th positions (peptide **VII**) destabilize the α-helical conformation, making these Ac_6c residues less effective in stabilizing the α-helix compared to those in other peptides listed in Table 1. Interestingly, the introduction of two consecutive Ac_6c residues in the middle of the Aib-based peptide (peptide **VIII**) enhanced α-helical preference more effectively than the corresponding peptide containing a single Ac_6c residue in the middle (peptide **IX**).

Synthesis and conformational analysis of the stapled peptide $1C_7$

Based on the previous study[39,40] and the DFT study discussed above, we chose Ac_6c and its piperidine analog, Api, to construct an optically inactive stapled α-helical nonapeptide. In this design, two Api residues were incorporated at the ith and i + 4th positions, namely the 3rd and 7th from the N-terminus, to be tethered by a minimal staple. Our modeling study suggested that a flexible cross-linker based on heptanedioic acid would be a minimal i, i + 4 staple suitable for cross-linking between the side chains of the Api residues incorporated at the i and i + 4 positions of the Ac_6c-based achiral peptide chain. The linear peptide, Z-$(Ac_6c)_2$-Api(Boc)-$(Ac_6c)_3$-Api(Boc)-Ac_6c-Aib-OMe (Z = benzyloxycarbonyl, Boc = *tert*-butoxycarbonyl, and OMe = methoxy), was prepared *via* stepwise liquid phase synthesis (Fig. 1a and Scheme S1†). After deprotection of the Boc groups at the Api side chains, the resulting peptide was reacted with the activated diester stapling reagent (**2**), containing a C_7 linker, in the presence of base under dilute conditions, affording the stapled peptide $\mathbf{1C_7}$ in moderate yield (Fig. 1a, see ESI† for more details). The stapled peptide $\mathbf{1C_7}$ was identified by electrospray ionization time-of-flight (ESI-TOF) mass spectrometry, and its purity was confirmed by high-performance liquid chromatography (HPLC) analysis (Fig. S1†).[43]

Interestingly, the ^{1}H NMR spectral pattern of $\mathbf{1C_7}$ in 1,1,2,2-tetrachloroethane-d_2 (TCE-d_2) at 298 K was complicated (Fig. 3), due to the presence of four possible side-chain amide carbonyl (–CO-N$(CH_2)_2$–) orientations: *endo*/*exo*, *exo*/*exo*, *exo*/*endo*, and *endo*/*endo* (Fig. 4). These orientations interconvert slowly on the NMR time scale, with *endo* and *exo* referring to their orientations relative to a plane passing through the midpoint of the two amide side chains and the center of the helix. This complexity is evident in the N-terminal urethane N(1)H proton signal, observed around 5.6 ppm, which appears as a dominant peak accompanied by three minor peaks. In contrast, previously reported α-helical peptides composed mainly of Ac_6c and Api residues with (i, i + 7) flexible hydrocarbon

Table 1 Effect of the number and position of Ac_6c residue in the optically inactive helical nonapeptides **I**–**IX** (acetyl-$(AA)_9$-$NHCH_3$, AA = Ac_6c and/or Aib) on the energy difference ($\Delta E_{\alpha\text{-}310}$ and $\Delta E_{\alpha\text{-}310}/n$, where $\Delta E_{\alpha\text{-}310} = E_{\alpha} - E_{310}$ and n = number of Ac_6c residues, in kJ mol^{-1}) between α- and 3_{10}-helical conformations[a]

	Amino acid sequence from N-terminus (1) to C-terminus (9)									
Peptide	1	2	3	4	5	6	7	8	9	$\Delta E_{\alpha\text{-}310}$ ($\Delta E_{\alpha\text{-}310}/n$) (kJ mol^{-1})
I	Aib	Ac_6c	Aib	Ac_6c	Aib	Ac_6c	Aib	Ac_6c	Aib	−1.72 (−0.41)
II	Aib	Ac_6c	Aib	Ac_6c	Aib	Ac_6c	Ac_6c	Ac_6c	Aib	−6.51 (−1.31)
III	Aib	Ac_6c	Aib	Ac_6c	Ac_6c	Ac_6c	Ac_6c	Ac_6c	Aib	−10.3 (−1.71)
IV	Aib	Ac_6c	Ac_6c	Ac_6c	Ac_6c	Ac_6c	Ac_6c	Ac_6c	Aib	−11.3 (−1.61)
V	Ac_6c	Ac_6c	Ac_6c	Ac_6c	Ac_6c	Ac_6c	Ac_6c	Ac_6c	Ac_6c	−15.1 (−1.67)
VI	Aib	Aib	Ac_6c	Aib	Aib	Ac_6c	Aib	Aib	Aib	−1.59 (−0.80)
VII	Aib	Aib	Ac_6c	Aib	Aib	Aib	Ac_6c	Aib	Aib	−0.51 (−0.25)
VIII	Aib	Aib	Aib	Aib	Ac_6c	Ac_6c	Aib	Aib	Aib	−2.42 (−1.21)
IX	Aib	Aib	Aib	Aib	Ac_6c	Aib	Aib	Aib	Aib	−0.56 (−0.56)

[a] The averaged dihedral angles ($|\phi|/|\psi|$) of all energy-minimized α- and 3_{10}-helical structures were varied within |56|/|45–48| and |54–56|/|30–32|, respectively.

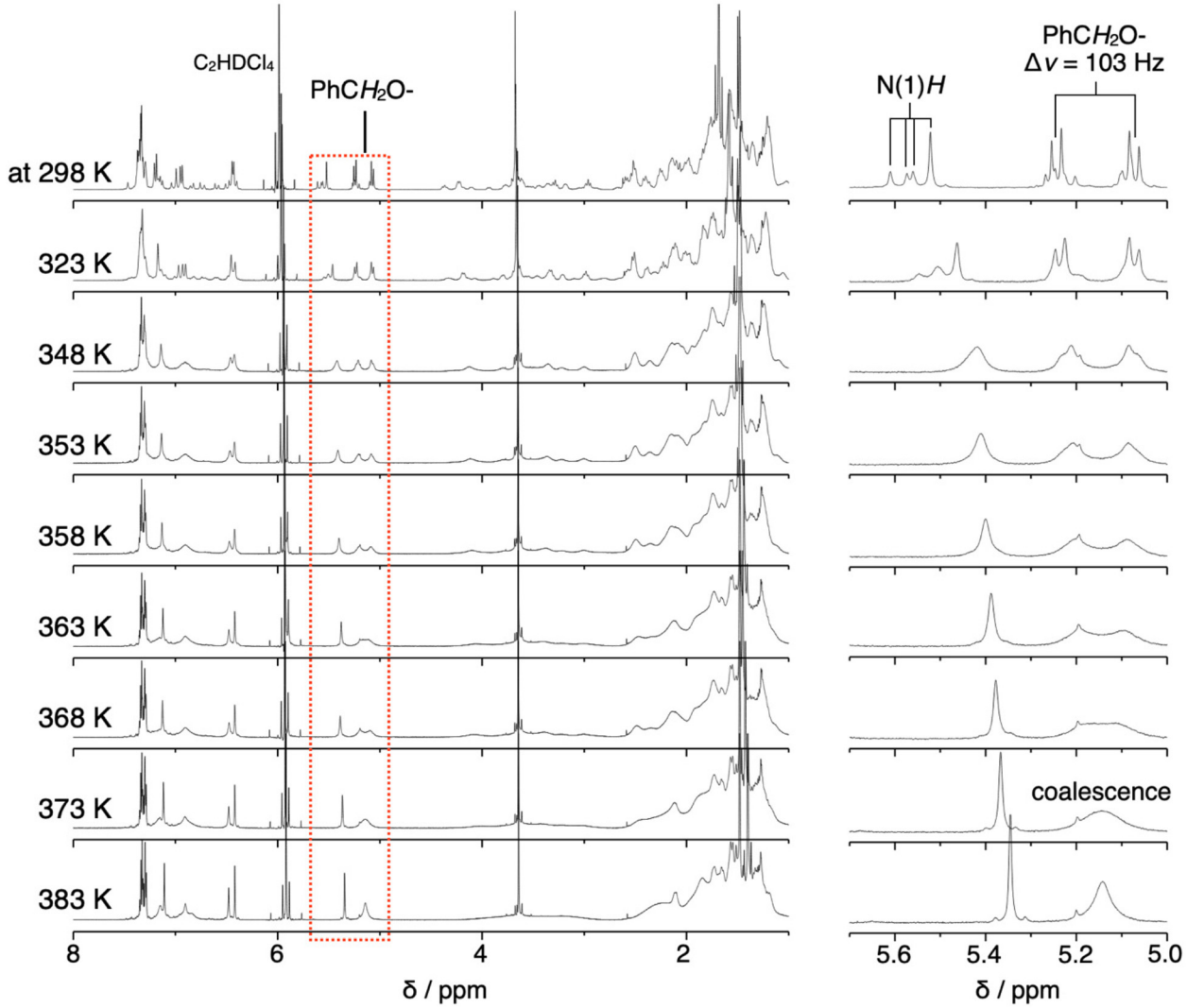

Fig. 3 Temperature-dependent ^{1}H NMR (600 MHz, $C_2D_2Cl_4$, 5.0 mM) spectral changes of **1C$_7$**. The expanded spectra of the highlighted region (indicated by the red dotted rectangle) is shown in the right panel, illustrating the temperature-dependent behavior of the N-terminal methylene protons and the amide N(1)H signals.

stapling exhibit only a single orientation (*exo*/*exo*).[40] DFT calculations of **1C$_7$** with these four amide carbonyl orientations suggest that the major conformation could be assigned to an α-helical conformation with the *endo*/*exo* amide carbonyl orientation (conf-1 in Fig. S2a†), which is the lowest energy conformation among them (Fig. S2†). This structural assignment is further supported by single-crystal X-ray diffraction, which reveals that **1C$_7$** adopts an α-helical conformation with the *endo*/*exo* orientation. The analyzed crystal contains two crystallographically independent but conformationally similar molecules, A and B, both of which adopt a typical α-helical conformation (average dihedral angles ($|\phi|/|\psi|$) excluding the C-terminal Aib residue: 57°/44° for A and 56°/46° for B) (Fig. 5). Interestingly, the amide NH groups of the Api(3) residues of these peptides adopt an axial orientation, whereas those of the Api(7) residues are found in an equatorial orientation (Fig. 4, left panel and 5). In addition, the energy difference (ΔE) between the energy-minimized structure obtained by DFT calculations using molecule B as an initial structure and the corresponding structure with all equatorial positions is only 2.2 kJ mol^{-1} (Fig. S2a and f†). This axial–equatorial conformational fluctuation is most likely due to the high flexibility of the stapling moiety.

The ^{1}H NMR spectrum of **1C$_7$** in TCE-d_2 at 298 K displayed diastereotopic splitting of the methylene protons of the N-terminal Z group ($\Delta\nu$ = 103 Hz), indicating that the interconversion between the (*P*) and (*M*)-helices is slow on the NMR time scale (Fig. 3). To estimate the free energy of activation ($\Delta G^{\ddagger}$, kJ mol^{-1}) for the *P*/*M* interconversion of **1C$_7$** at the coalescent temperature (T_c) of the signal splitting of the methylene protons, we performed variable-temperature ^{1}H NMR measurements. As the temperature increased from 298 K to 348 K, the four N(1)H signals, corresponding to the different side chain amide carbonyl orientations, gradually

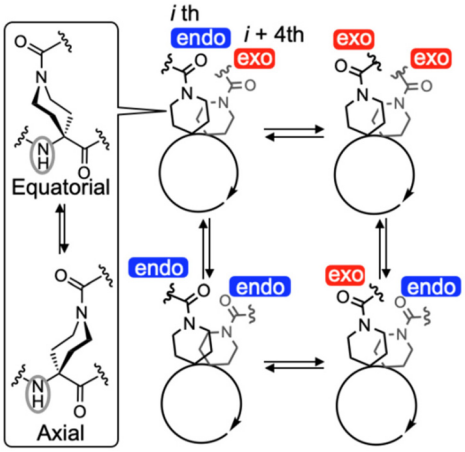

Fig. 4 Schematic representation of the interconversions between four possible orientations (*endo* or *exo*) of the side-chain amide carbonyl (–CO-N(CH_2)–) groups on the Api residues in the (*P*)-α-helical **1C$_7$**. Here, *endo* and *exo* represent their orientations relative to a plane passing through the midpoint of the two amide side chains and the center of the helix. Additionally, the interconversion between the equatorial and axial positions of the amide NH group on the piperidine ring of the Api residue is also show.

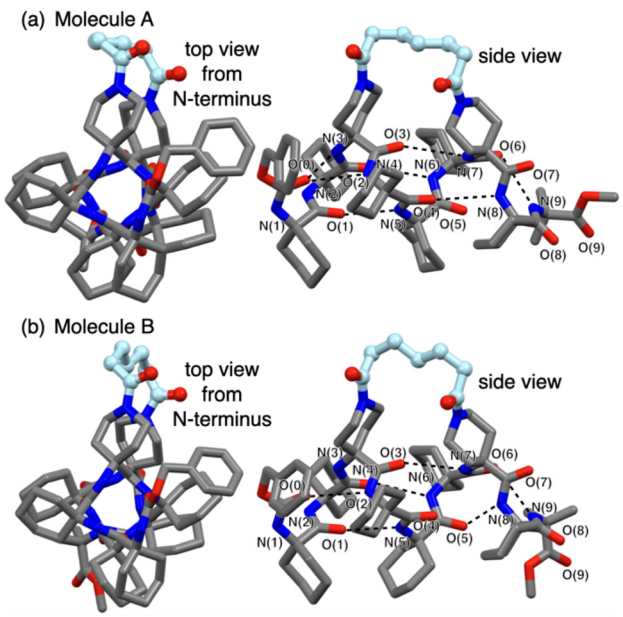

Fig. 5 The X-ray crystal structures of (*P*)-α-helical **1C$_7$**. Crystallographically independent molecules A (a) and B (b) are shown. Only the (*P*)-helix is shown. All of the hydrogen atoms, disordered atoms and solvent molecules are omitted for clarity. Dotted lines represent intramolecular hydrogen bonds. The dihedral angles (ϕ, ψ and ω) and hydrogen-bonding parameters of **1C$_7$** are summarized in Tables S13 and S16.† The number in parentheses represents the residue number from the N-terminus.

broadened and coalesced. However, the N-terminal methylene proton signals remained split throughout this temperature range, indicating that the *P*/*M* interconversion is much slower than the interconversion between these four conformers. At 373 K, the methylene proton signals finally coalesced, giving the $\Delta G^{\ddagger}$ value of 75.2 kJ mol^{-1}. The rate constants (k, sec^{-1}) for the *P*/*M* interconversion were estimated to be 229 s^{-1} at T_c and 0.41 s^{-1} at 298 K using the equation $k = (k_B T/h)\exp(-\Delta G^{\ddagger}/RT)$. Surprisingly, the k_{298} value of **1C$_7$** is approximately 10^2 times faster than that of a previously reported α-helical peptide with a rigid (i, i + 7) biphenyl-based staple, which has only a single set of the amide carbonyl orientations on the Api side chains.[39] This suggests that the rigidity of the stapling moiety plays a crucial role in restricting the overall conformational flexibility of the peptide including intermediate structures during the helix reversal process.

Conclusions

We have successfully designed and synthesized a dynamically optically inactive α-helical peptide foldamer composed mainly of achiral Ac_6c and Api residues with an (i, i + 4) hydrocarbon-based staple. While this single staple effectively slowed the *P*/*M* interconversion rate of the peptide, it did not significantly restrict the conformational freedom of the Api side-chain amide carbonyl linked by the staple. Furthermore, in helical oligopeptides composed mainly of Aib and Ac_6c residues, we found that Ac_6c promotes α-helical formation more strongly than Aib, favoring the α-helix over the 3_{10}-helix in a highly position-dependent manner. This α-helical propensity is further enhanced when a segment contains more than three consecutive Ac_6c residues within the oligopeptides. Our findings may provide not only a deeper understanding of how staple length and rigidity influence α-helical stability, but also a rational design strategy for unique helical peptides capable of stimuli-responsive 3_{10}/α-helix transitions and tunable *P*/*M* interconversion rates.

Author contributions

N.O. conceived the project, designed and performed the experiments, analysed the data, and wrote the paper. S.A. performed X-ray crystallographic analysis. All authors discussed the results and commented on the manuscript.

Data availability

The data supporting this article have been included as part of the ESI.† Additional data are available upon request from the authors. Crystallographic data for compound **1C$_7$** have been deposited at the Cambridge Crystallographic Data Centre [CCDC 2421064].†

Conflicts of interest

There are no conflicts to declare.

Acknowledgements

This work was supported in part by JSPS KAKENHI (JP22K05220 (N. O.)) and the World Premier International Research Center Initiative (WPI), MEXT, Japan (N. O., S. A., and M. J. M.).

References

1 G. L. Verdine and G. J. Hilinski, *Methods Enzymol.*, 2012, **503**, 3–33.
2 A. M. Ali, J. Atmaj, N. Van Oosterwijk, M. R. Groves and A. Dömling, *Comput. Struct. Biotechnol. J.*, 2019, **17**, 263–281.
3 R. Mourtada, H. D. Herce, D. J. Yin, J. A. Moroco, T. E. Wales, J. R. Engen and L. D. Walensky, *Nat. Biotechnol.*, 2019, **37**, 1186–1197.
4 H. Yokoo, M. Hirano, T. Misawa and Y. Demizu, *ChemMedChem*, 2021, **16**, 1226–1233.
5 Y. Li, M. Wu, Y. Fu, J. Xue, F. Yuan, T. Qu, A. N. Rissanou, Y. Wang, X. Li and H. Hu, *Pharmacol. Res.*, 2024, **203**, 107137.
6 L. D. Walensky, A. L. Kung, I. Escher, T. J. Malia, S. Barbuto, R. D. Wright, G. Wagner, G. L. Verdine and S. J. Korsmeyer, *Science*, 2004, **305**, 1466–1470.
7 Y. H. Lau, P. De Andrade, Y. T. Wu and D. R. Spring, *Chem. Soc. Rev.*, 2015, **44**, 91–102.
8 X. Li, S. Chen, W. D. Zhang and H. G. Hu, *Chem. Rev.*, 2020, **120**, 10079–10144.
9 S. Hecht and A. Khan, *Angew. Chem., Int. Ed.*, 2003, **42**, 6021–6024.
10 K. Maeda, H. Mochizuki, M. Watanabe and E. Yashima, *J. Am. Chem. Soc.*, 2006, **128**, 7639–7650.
11 A. Hashimoto, H. Sogawa, M. Shiotsuki and F. Sanda, *Polymer*, 2012, **53**, 2559–2566.
12 N. Fuentes, A. Martin-Lasanta, L. Alvarez de Cienfuegos, R. Robles, D. Choquesillo-Lazarte, J. M. García-Ruiz, L. Martínez-Fernández, I. Corral, M. Ribagorda, A. J. Mota, D. J. Cárdenas, M. C. Carreño and J. M. Cuerva, *Angew. Chem., Int. Ed.*, 2012, **51**, 13036–13040.
13 C. Tsiamantas, X. de Hatten, C. Douat, B. Kauffmann, V. Maurizot, H. Ihara, M. Takafuji, N. Metzler-Nolte and I. Huc, *Angew. Chem., Int. Ed.*, 2016, **55**, 6848–6852.
14 L. Zheng, C. Yu, Y. Zhan, X. Deng, Y. Wang and H. Jiang, *Chem. – Eur. J.*, 2017, **23**, 5361–5367.
15 H. Abe, C. Sato, Y. Ohishi and M. Inouye, *Eur. J. Org. Chem.*, 2018, 3131–3138.
16 N. Miki, R. Inoue and Y. Morisaki, *Bull. Chem. Soc. Jpn.*, 2021, **95**, 110–115.
17 I. L. Karle and P. Balaram, *Biochemistry*, 1990, **29**, 6747–6756.
18 C. Toniolo and E. Benedetti, *Trends Biochem. Sci.*, 1991, **16**, 350–353.
19 C. Toniolo, M. Crisma, F. Formaggio and C. Peggion, *Biopolymers*, 2001, **60**, 396–419.
20 M. Tanaka, *Chem. Pharm. Bull.*, 2007, **55**, 349–358.
21 M. Crisma and C. Toniolo, *Biopolymers*, 2015, **104**, 46–64.
22 N. Shamala, R. Nagaraj and P. Balaram, *J. Chem. Soc., Chem. Commun.*, 1978, 996–997.
23 V. Moretto, M. Crisma, G. M. Bonora, C. Toniolo, H. Balaram and P. Balaram, *Macromolecules*, 1989, **22**, 2939–2944.
24 P. K. C. Paul, M. Sukumar, R. Bardi, A. M. Piazzesi, G. Valle, C. Toniolo and P. Balaram, *J. Am. Chem. Soc.*, 1986, **108**, 6363–6370.
25 M. Crisma, G. M. Bonora, C. Toniolo, A. Bavoso, E. Benedetti, B. Di Blasio, V. Pavone and C. Pedone, *Macromolecules*, 1988, **21**, 2071–2074.
26 V. Pavone, E. Benedetti, V. Barone, B. Di Blasio, F. Lelj, C. Pedone, A. Santini, M. Crisma, G. M. Bonora and C. Toniolo, *Macromolecules*, 1988, **21**, 2064–2070.
27 C. L. Wysong, T. S. Yokum, G. A. Morales, R. L. Gundry, M. L. McLaughlin and R. P. Hammer, *J. Org. Chem.*, 1996, **61**, 7650–7651.
28 T. S. Yokum, T. J. Gauthier, R. P. Hammer and M. L. McLaughlin, *J. Am. Chem. Soc.*, 1997, **119**, 1167–1168.
29 Y. Paterson, S. M. Rumsey, E. Benedetti, G. Nemethy and H. A. Scheraga, *J. Am. Chem. Soc.*, 1981, **103**, 2947–2955.
30 C. Toniolo, M. Crisma, G. M. Bonora, E. Benedetti, B. Dl Blasio, V. Pavone, C. Pedone and A. Santini, *Biopolymers*, 1991, **31**, 129–138.
31 P. Kumar, N. G. Paterson, J. Clayden and D. N. Woolfson, *Nature*, 2022, **607**, 387–392.
32 R.-P. Hummel, C. Toniolo and G. Jung, *Angew. Chem., Int. Ed. Engl.*, 1987, **26**, 1150–1152.
33 M. Kubasik and A. Blom, *ChemBioChem*, 2005, **6**, 1187–1190.
34 M. Kubasik, J. Kotz, C. Szabo, T. Furlong and J. Stace, *Biopolymers*, 2005, **78**, 87–95.
35 J. Clayden, A. Castellanos, J. Solà and G. A. Morris, *Angew. Chem., Int. Ed.*, 2009, **48**, 5962–5965.
36 B. A. F. Le Bailly and J. Clayden, *Chem. Commun.*, 2016, **52**, 4852–4863.
37 N. Ousaka, T. Sato and R. Kuroda, *J. Am. Chem. Soc.*, 2008, **130**, 463–465.
38 N. Ousaka, Y. Inai and R. Kuroda, *J. Am. Chem. Soc.*, 2008, **130**, 12266–12267.
39 N. Ousaka, M. J. MacLachlan and S. Akine, *Nat. Commun.*, 2023, **14**, 6834.
40 N. Ousaka, M. J. MacLachlan and S. Akine, *Chem. – Eur. J.*, 2024, **30**, e202402704.
41 F. Mamiya, N. Ousaka and E. Yashima, *Angew. Chem., Int. Ed.*, 2015, **54**, 14442–14446.
42 N. Ousaka, Y. Takeyama and E. Yashima, *Chem. – Eur. J.*, 2013, **19**, 4680–4685.
43 We did not perform CD measurements of the stapled peptide $\mathbf{1C_7}$ to distinguish between α- and 3_{10}-helical conformations, as $\mathbf{1C_7}$ is composed solely of achiral components. Consequently, CD spectroscopy would not provide meaningful information in this case. Instead, the distinction between α- and 3_{10}-helices was determined using a combination of DFT calculations, X-ray crystallographic analysis, and temperature-dependent ^{1}H NMR data (for a detailed discussion, see the main text).